International Journal of Nanomedicine

Dovepress
open access to scientific and medical research

Open Access Full Text Article

ORIGINAL RESEARCH

Involvement of autophagy in tantalum nanoparticle-induced osteoblast proliferation

This article was published in the following Dove Press journal:
International Journal of Nanomedicine
7 June 2017
Number of times this article has been viewed

Chengrong Kang[1,2]
Limin Wei[1]
Bin Song[1]
Liangjiao Chen[3]
Jia Liu[1]
Bin Deng[4]
Xuan Pan[2]
Longquan Shao[1]

[1]Department of Stomatology, Nanfang Hospital, Southern Medical University, [2]Department of Stomatology, The First Affiliated Hospital of Guangdong Pharmaceutical University, [3]Department of Orthodontics, Key Laboratory of Oral Medicine, Guangzhou Institute of Oral Disease, Stomatology Hospital of Guangzhou Medical University, Guangzhou, [4]Department of Stomatology, The General Hospital of People's Liberation Army, Beijing, China

Abstract: Porous tantalum (Ta) implants are highly corrosion resistant and biocompatible, and they possess significantly better initial stability than that of conventional titanium (Ti) implants. During loading wear, Ta nanoparticles (Ta-NPs) that were deposited on the surface of a porous Ta implant are inevitably released and come into direct contact with peri-implant osteoblasts. The wear debris may influence cell behavior and implant stabilization. However, the interaction of Ta-NPs with osteoblasts has not been clearly investigated. This study aimed to investigate the effect of Ta-NPs on cell proliferation and their underlying mechanism. The Cell Counting Kit-8 (CCK-8) assay was used to measure the cell viability of MC3T3-E1 mouse osteoblasts and showed that Ta-NP treatment could increase cell viability. Then, confocal microscopy, Western blotting, and transmission electron microscopy were used to confirm the autophagy induced by Ta-NPs, and evidence of autophagy induction was observed as positive LC3 puncta, high-LC3-II expression, and autophagic vesicle ultrastructures. The CCK-8 assay revealed that the cell viability was further increased and decreased by the application of an autophagy inducer and inhibitor, respectively. In addition, pre-treatment with autophagy inhibitor 3-methyladenine (3-MA) inhibited the Ta-NP-induced autophagy. These results indicate that the Ta-NPs can promote cell proliferation, that an autophagy inducer can further strengthen this effect and that an autophagy inhibitor can weaken this effect. In conclusion, autophagy was involved in Ta-NP-induced cell proliferation and had a promoting effect.

Keywords: tantalum nanoparticles, osteoblast, autophagy, proliferation

Introduction

Early healing, early loading, and long-term biocompatibility are favorable characteristics of medical implant materials used in orthopedics and dentistry. Conventional titanium (Ti) implants have several disadvantages, such as an excessively long healing time due to poor early stability and insufficient stress conduction due to elastic modulus differences, which greatly influence the early healing, early loading, and long-term success of implants. Compared with Ti implants, tantalum (Ta) implants induce greater proliferation and differentiation and exhibit better bioactivity and cell–implant interactions.[1,2] Balla et al[3] compared the performance of porous Ta and porous Ti and discovered that porous Ta, because of its high wettability and greater surface energy, could better promote early biological fixation and showed excellent adherence, growth, and differentiation with abundant extracellular matrix formation. This study has provided direct evidence that Ta materials are superior to Ti materials with an identical porous structure.

Recently, Ta metal has received increasing interest as an implant material for load-bearing orthopedic applications owing to its excellent biocompatibility, corrosion resistance, and superior strength. Nanostructured Ta films have not only improved the

Correspondence: Longquan Shao
Department of Stomatology, Nanfang Hospital, Southern Medical University, 1838 North Guangzhou Road, Guangzhou 510515, China
Tel +86 20 6278 7153
Fax +86 20 6164 1101
Email shaolongquan@smu.edu.cn

Xuan Pan
Department of Stomatology, The First Affiliated Hospital of Guangdong Pharmaceutical University, 19 Nonglinxialu, Guangzhou 510080, China
Tel/fax +86 20 6132 5457
Email panxuan@tom.com

submit your manuscript | www.dovepress.com
Dovepress
http://dx.doi.org/10.2147/IJN.S136281

initial adhesion and spreading of cells but also exhibited good antibacterial activities.[4] Studies have demonstrated that Ta is a good substrate for the attachment, proliferation, and differentiation of osteoblasts.[5,6] However, the significantly high elastic modulus and high manufacturing cost have limited the wide application of Ta. As a potential solution to these issues, porous Ta, a Ta material with a modified structure, has been developed. Porous Ta has been manufactured by coating Ta nanoparticles (Ta-NPs) onto a low-density vitreous carbon scaffold via carbon vapor deposition and infiltration.[7,8] Porous Ta, also called porous Ta trabecular metal (PTTM), contains a co-adjacent vesicular framework that is similar to cancellous bone with pore sizes ranging from 300 to 600 μm and a porosity of 75%–85%, and its elastic modulus (1.3–10 GPa) is similar to that of natural cortical (12–18 GPa) and cancellous bone (0.1–0.5 GPa).[9] Porous Ta is non-toxic, highly corrosion resistant, biocompatible, and bioactive;[10] it allows both bone ingrowth and ongrowth and promotes osteogenesis to establish osseointegration and osseoincorporation, thus significantly enhancing the initial stability of implants[9,11] and the applicability to osteo-regenerative strategies.[12] Currently, porous Ta has been widely applied in orthopedic applications and oral implants, and studies have shown that it can highly promote the adhesion, proliferation, differentiation, and mineralization of osteoblasts in vitro[3,13,14] and in vivo.[15,16] In addition, recent studies have revealed that porous Ta combined with bone marrow stromal stem cells (BMSCs),[17] bone marrow mesenchymal stem cells (BMMSCs),[18] and fibrin[19] can better promote cell proliferation, bone integration, and regeneration.[20]

Currently, a commercial PTTM-enhanced Ti dental implant is applied. The PTTM material was added as an unthreaded sleeve to the midsection of the conventional tapered, root form Ti dental implant. The cervical, apical, and internal structures of the implant are composed of a Ti alloy.[8,21] These PTTM-enhanced implants provide clinicians with an alternative option for immediate placement and early loading. Schlee et al[22] conducted a proof-of-principle study to evaluate the clinical efficacy of immediately loading PTTM implants. Implants were placed in premolar or molar locations of healthy, partially edentulous patients and were given immediate occlusal loading. After 1 year of clinical follow-up, the implants achieved 100% (n=22/22) survival with no serious complications. The findings indicated that the PTTM implant was safe and effective for immediate loading under controlled clinical conditions. Meanwhile, Schlee et al[21] conducted another 1-year prospective, multicenter trial at 22 clinical sites of five European countries and revealed that the survival rate of the PTTM implant was 95.2% (n=138/145). The authors concluded that PTTM dental implants were clinically effective under various uncontrolled clinical conditions.

During loading wear, coating particles may be liberated from the implant surface and interact with local cells, resulting in a complex local cellular response that may influence the balance between bone formation and resorption.[23] Zhu et al[4] reported a release of <2 μg/L Ta from Ta films deposited on sand-blasted, large grit, and acid etched (SLA) Ti surfaces after immersion in PBS for 28 days. Bonutti et al[24] reported a case of metallosis following a total knee arthroplasty (TKA) that used a porous Ta tibial knee component. The patient's operation employed a revised TKA, and delamination of the tibial component was found. Around the delaminated porous Ta tibial component, the soft tissue was discolored to a grayish hue; an analysis for metal particles was performed, revealing that the composition was consistent with that of the porous Ta baseplate. The extra-articular migration of Ta particles indicated regional dissemination of the metal. Wear particles, as small as 50 nm,[25] could be taken up but not digested by cells, thus inducing intracellular stress. This intracellular stress potently further induces a series of cellular responses including autophagy, which may be an attempt to degrade the wear particles.[26,27] Autophagy, an evolutionarily conserved process in which damaged organelles, intracellular pathogens, and endocytic extracellular materials are degraded and recycled, plays an important role in the response to environmental stimuli and is important for cells to overcome or adapt to adverse conditions.[28]

As the wear debris which is liberated from the surface of PTTM implants during loading wear, Ta-NPs may be taken up by osteoblasts and induce intracellular stress. As some of the first cells exposed to wear debris, osteoblasts play an important role in the balance of bone metabolism.[29] However, the interaction of Ta-NPs with osteoblasts and their underlying mechanism have not been clearly investigated. On the basis of the abovementioned studies, we hypothesize that autophagy may be the targeted cellular response through which osteoblasts degrade Ta-NPs and overcome harmful conditions.

In this study, the mouse osteoblast cell line MC3T3-E1 was used to study the effect of Ta-NPs on cell proliferation and investigate the involvement and role of autophagy.

Materials and methods

Chemicals

The Ta-NPs were purchased from Sigma-Aldrich (St Louis, MO, USA; product number 593486). Antibodies

against LC3B, sequestosome-1/p62 (SQSTM1/p62), β-actin, and goat anti-rabbit IgG were purchased from Cell Signaling Technology (CST, Beverly, MA, USA). The autophagy inducer rapamycin and the autophagy inhibitor 3-methyladenine (3-MA) were obtained from Sigma-Aldrich. The Cell Counting Kit-8 (CCK-8, Dojindo, Japan) assay was used to evaluate cell viability.

Chemical suspensions

One milligram of Ta-NPs was packed into a sterile tube and sterilized with 25 kGy of cobalt-60 irradiation. Next, 1 mL of alpha-modified Eagle's medium (α-MEM) was added to the tube, which was then sonicated for 3 min (9×20 s, 160 W, 20 kHz) at room temperature to prepare a 1 mg/mL homogeneous Ta-NP suspension. This suspension was serially diluted with α-MEM and sonicated as above to obtain working Ta-NP suspensions. All the Ta-NP suspensions were freshly prepared before use. Rapamycin and 3-MA were dissolved according to the manufacturer's instructions to form stock solutions, which were frozen at −20°C until use. The stock solutions were diluted to working concentrations with α-MEM when needed.

Cell culture

The mouse osteoblast cell line MC3T3-E1 was purchased from the Cell Bank of the Shanghai Institute of Life Sciences (Chinese Academy of Sciences, Beijing, China). Cells were cultured in α-MEM (Thermo Fisher Scientific, Waltham, MA, USA) supplemented with 10% fetal bovine serum (Thermo Fisher Scientific), and 1% penicillin/streptomycin (Thermo Fisher Scientific) at 37°C in a humidified atmosphere containing 5% CO_2. After achieving adherence after 24 h, cells were exposed to the Ta-NPs at different concentrations with or without pretreatment with rapamycin or 3-MA. Cells cultured in α-MEM alone were used as a negative control.

Cell viability using the CCK-8 assay

The MC3T3-E1 cells were seeded in 96-well plates (Costar, USA) at a density of 1×10^3 cells/well with 100 μL of α-MEM for 24 h. After cell adhesion was achieved, the culture medium was replaced with specific chemical suspensions. Then, the cells were incubated for another 24 h. At specific time points, the plates were washed three times with PBS, and 100 μL of fresh α-MEM and 10 μL of CCK-8 reagent were added. After a 2 h incubation, the absorbance of the supernatant at 540 nm was quantified using a multi-well plate reader (Multiskan GO; Thermo Fisher Scientific) to evaluate cell viability. The relative viability of the cells was calculated using the following formula: relative viability = [(As−Ab)/(Ac−Ab)]×100%, where As is the experimental OD, Ac is the control OD, and Ab is the blank OD. At least three wells per condition were examined in three independent experiments. To evaluate the effect of Ta-NPs on cell proliferation, the culture medium was replaced with 0, 1, 10, and 20 μg/mL Ta-NP suspensions. To explore the involvement and role of autophagy, cells were treated with rapamycin or 3-MA for 1 h followed by Ta-NP treatment or not, and cells treated with α-MEM alone were used as a negative control.

Autophagosome images by confocal immunofluorescence microscopy

MC3T3-E1 cells were cultured in a 20 μg/mL Ta-NP suspension with or without pretreatment with 3-MA for the experimental groups, in α-MEM alone for the negative control group, and in 200 nM rapamycin for the positive control group. After cells adhesion was achieved, the culture medium was replaced as described above, and the cells were incubated for another 24 h. At the time indicated, the cells were incubated with antibodies against LC3B (1:200, rabbit antibodies) at 37°C for 60 min to label the autophagosomes and then washed and incubated with α-MEM at 37°C for 30 min. The culture medium was then removed, and the cells were loaded with 70 nM LysoTracker Red DND-99 at 37°C for 1 h to label the lysosomes. Finally, the cell nuclei were loaded with Hoechst 33342 at 37°C for 20 min. Before an observation was performed, the cells were washed and sealed with anti-fade mounting medium (Beyotime, Beijing, China). All the fluorescence measurements were recorded using an FV10i confocal microscope (Olympus, Tokyo, Japan). LysoTracker Red DND-99 and Hoechst 33342 were purchased from Invitrogen (Thermo Fisher Scientific).

Expression of autophagy proteins in the Western blots

The MC3T3-E1 cells were seeded in 10 cm cell culture dishes (Thermo Fisher Scientific) at a density of 1×10^4 cells/dish with 10 mL of α-MEM for 24 h. After the cell adhesion was achieved, the culture medium was replaced with either a 20 μg/mL Ta-NP suspension, with or without pretreatment with 3-MA, as experimental groups, or α-MEM alone as the negative control group, and 200 nM rapamycin as the positive control group, and the cells were incubated for another 24 h. At the indicated time, cells were lysed with lysis buffer (Whole Cell Lysis Assay, Keygen, China), and the cell lysates were centrifuged at 10,000× *g* for 10 min at 4°C. The supernatants were analyzed using a

BCA Protein Quantitation Assay (Beyotime). Equivalent protein lysates were loaded onto sodium dodecyl sulfate-polyacrylamide gels and electrophoretically transferred to polyvinylidene fluoride membranes (Merck Millipore, Billerica, MA, USA) using a Trans-Blot Turbo Transfer System (Bio-Rad, Hercules, CA, USA). The membranes were rinsed three times with 1× Tris-buffered saline containing 0.05% Tween-20. After blocking with 5% nonfat milk, the membranes were incubated with primary antibodies against LC3B, p62, and β-actin (1:1,000, rabbit antibodies) overnight at 4°C and then washed and incubated with a horseradish peroxidase-conjugated secondary antibody (1:2,000, anti-rabbit antibodies) for 1 h at room temperature. The antibody-bound proteins were detected using a Pierce ECL Western blot substrate (Thermo Fisher Scientific). The protein bands were analyzed using Image Lab software (Bio-Rad).

Ultrastructure of autophagic vesicles determined by transmission electron microscopy

The MC3T3-E1 cells were seeded in 6-well plates (Costar) at a density of 4×10^3 cells/well with 3 mL of α-MEM for 24 h. After the cell adhesion was achieved, the culture medium was replaced with either a 20 μg/mL Ta-NP suspension, with or without pretreatment with 3-MA, as experimental groups, or a 200 nM rapamycin as the positive control group, and the cells were incubated for another 24 h. At the end of the incubation, the cells were washed twice with PBS, detached from the dishes using a cell scraper and centrifuged at 1,000× *g* for 5 min at room temperature. The cell pellets collected were fixed in 2.5% glutaraldehyde at room temperature for 1 h and then at 4°C for 3 h. The samples were post-fixed in 1.3% osmium tetroxide for 1 h, dehydrated in graded ethanol, and then embedded. Ultrathin sections were prepared and mounted on 3 mm, 200-mesh copper grids. The grids were examined and photographed with a Hitachi H-7500 TEM instrument (Hitachi, Japan).

Statistical analysis

All the quantitative results are presented as the mean ± standard deviation. The data were normalized, and those that passed the normality test were analyzed using one-way analysis of variance with the least significant difference test; those that did not pass the normality test were analyzed using Dunnett's test. All analyses were conducted using SPSS 22.0 software (SPSS Inc., Chicago, IL, USA). Statistical significance was considered for *P*-values <0.05.

Results

Characterization of Ta-NPs

We first characterized the physical properties of the Ta-NPs. Transmission electron microscopy (TEM; Mic JEM-1011, JEOL, Japan) and scanning electron microscopy (Nova Nano 430, FEI, Finland) were used to observe the size and shape of the Ta-NPs, which were primarily spherical with a mean particle diameter of 8–15 nm (Figure 1A and B). The hydrodynamic measurements of the Ta-NPs were conducted using dynamic light scattering (Malvern Instruments Ltd., Malvern, UK, DTS Ver. 5.10; serial number: MAL1016070; Figure 1C). The results showed that the Ta-NPs exhibited a hydrodynamic size of 292 nm with a mean peak intensity of 261 nm, corresponding to 100% of the total particle intensity.

Effect of Ta-NPs on cell proliferation

The CCK-8 assay was used to measure the cell viability and to evaluate the effect of the Ta-NPs on cell proliferation. The relative cell viability is displayed in Figure 2. As shown, the cell viability of all the Ta-NP-treated groups was higher than that of the control group, especially for the 10 and 20 μg/mL groups ($P<0.05$), with 20% and 18.7% increases in cell viability, respectively. These results revealed that the Ta-NPs can promote the proliferation of MC3T3-E1 osteoblasts.

Effect of autophagy on cell proliferation

To further investigate the involvement of autophagy and its effect on cell proliferation, an autophagy inducer (rapamycin) and autophagy inhibitor (3-MA) were used in the CCK-8 assay to measure the cell viability. MC3T3-E1 cells were cultured with 10 and 20 μg/mL Ta-NPs for 24 h, with or without pretreatment with rapamycin (200 nM) or 3-MA (10 mM) for 1 h (Figure 3). Cells were also treated with rapamycin or 3-MA alone to examine whether the autophagy regulators have an additional effect on cell viability. It was revealed that rapamycin or 3-MA alone had no obvious influence on cell viability. When cells were cultured with 10 μg/mL Ta-NPs, pretreatment with rapamycin and 3-MA slightly increased and decreased the cell viability, respectively ($P<0.05$), while the viability of cells pretreated with 3-MA was obviously lower than that of cells pretreated with rapamycin ($P<0.01$). When the cells were cultured with 20 μg/mL Ta-NPs, the viability of the cells pretreated with 3-MA decreased to ~50% and was significantly lower than that for the other two groups ($P<0.001$), while the cell viability between groups pretreated with or without rapamycin was not significantly different ($P>0.05$). Thus, autophagy regulators alone had no obvious influence on cell viability. When the cells were cultured

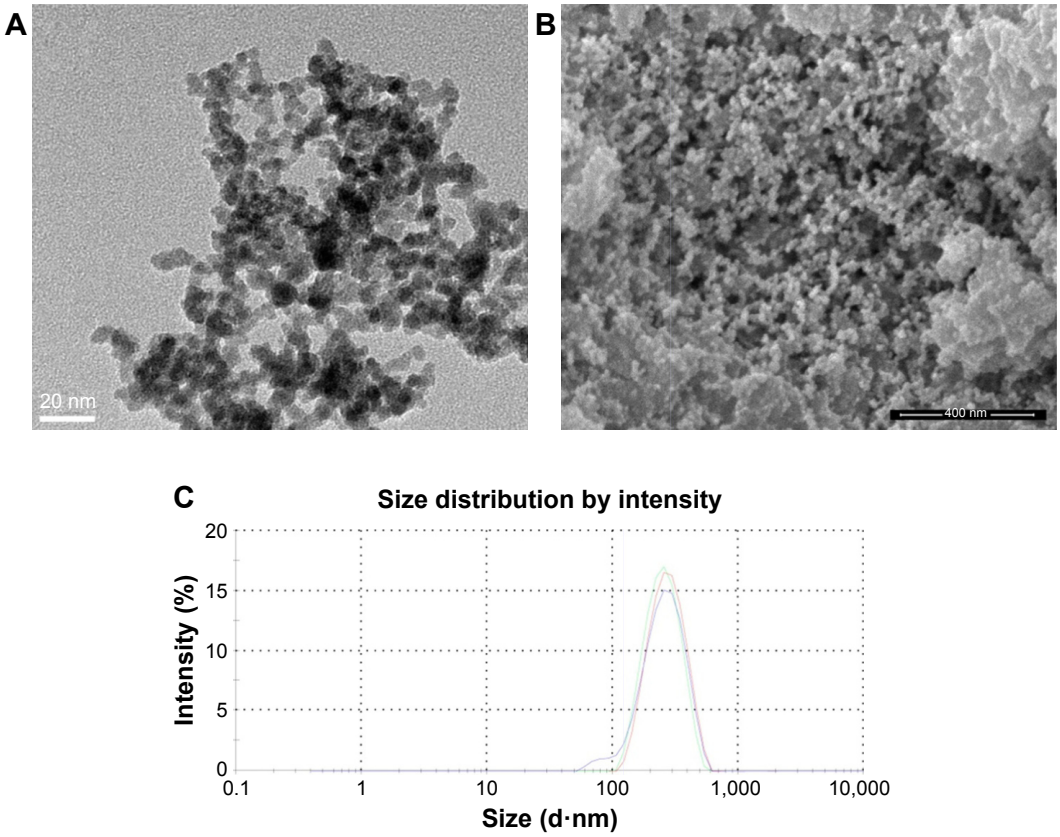

Figure 1 Characterization of Ta-NPs. TEM (**A**) and SEM (**B**) images showing primarily spherical shapes. Magnification ×200,000. (**C**) DLS measurements. The red, green and blue lines indicate three independent experiments.
Abbreviations: DLS, dynamic light scattering; SEM, scanning electron microscopy; Ta-NPs, Ta nanoparticles; TEM, transmission electron microscopy.

with Ta-NPs, autophagy induction further increased cell viability, while autophagy inhibition decreased cell viability, revealing that autophagy can promote the proliferation of MC3T3-E1 cells.

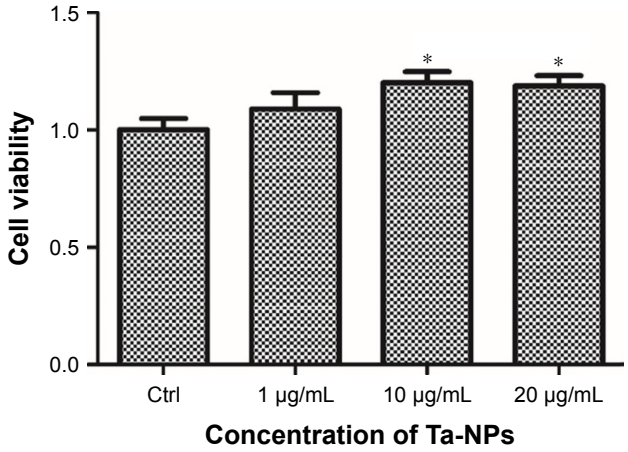

Figure 2 Cell viability of MC3T3-E1. The MC3T3-E1 cells were cultured with Ta-NPs at 1, 10, or 20 μg/mL for 24 h; cells cultured with α-MEM alone served as a control. The cell viability of all the Ta-NP-treated groups was higher than that of the control group, especially for the 10 and 20 μg/mL groups ($P<0.05$). Experiments were repeated three times with at least three wells per condition.
Note: *$P<0.05$ versus control group.
Abbreviations: α-MEM, alpha-modified Eagle's medium; Ta-NPs, Ta nanoparticles.

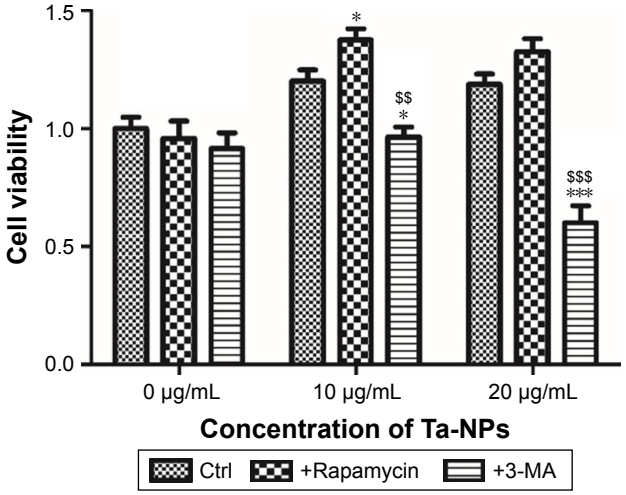

Figure 3 Cell viability of MC3T3-E1. MC3T3-E1 cells were cultured with 10 and 20 μg/mL Ta-NPs for 24 h, with or without pretreatment with rapamycin (200 nM) or 3-MA (10 mM) for 1 h; cells were also treated with rapamycin or 3-MA alone to identify whether they have an effect on cell viability.
Notes: The pretreatment with rapamycin and 3-MA accordingly increased and decreased the cell viability, respectively. Especially, the 20 μg/mL group pretreated with 3-MA had decreased cell viability of nearly 50%. These results showed that rapamycin or 3-MA alone had no obvious influence on cell viability, while autophagy induction further increased cell viability and autophagy inhibition decreased cell viability. Experiments were repeated three times with at least three wells per condition. *$P<0.05$, ***$P<0.001$ versus control group; $^{\$\$}P<0.01$, $^{\$\$\$}P<0.001$ versus rapamycin-pretreated group.
Abbreviations: 3-MA, 3-methyladenine; Ta-NPs, Ta nanoparticles.

Autophagy detection

As we demonstrated that autophagy promotes Ta-NP-induced cell proliferation, we next confirmed the autophagy induction by Ta-NPs in MC3T3-E1 cells and observed the change in autophagy flux upon pretreatment with an autophagy inhibitor. The MC3T3-E1 cells were cultured with 20 μg/mL Ta-NPs for 24 h with or without pretreatment with 3-MA (10 mM) for 1 h; cells treated with α-MEM alone served as a negative control group, and cells treated with 200 nM rapamycin served as a positive control group.

Accumulation of autophagosomes

An FV10i confocal microscope was used to observe the autophagosomes labeled with an LC3 fluorescent dye. The LC3 antibodies formed puncta (a characteristic of autophagosomes) and were labeled with a green color, the LysoTracker Red DND-99 dye-labeled lysosomes with a red color, and Hoechst 33342-labeled cell nuclei with a blue color (Figure 4). The green puncta could be clearly observed in the positive control group but were nearly indistinguishable in the negative control group, which indicated an effective induction of autophagy and a low level of basal autophagy in the MC3T3-E1 cells. Moreover, the green puncta in the 20 μg/mL Ta-NP-treated group were even more numerous than in the positive control group, indicating significant upregulation of autophagy by 20 μg/mL Ta-NPs. In contrast, pretreatment with 3-MA sharply decreased the amount of green puncta compared with the group treated with Ta-NPs

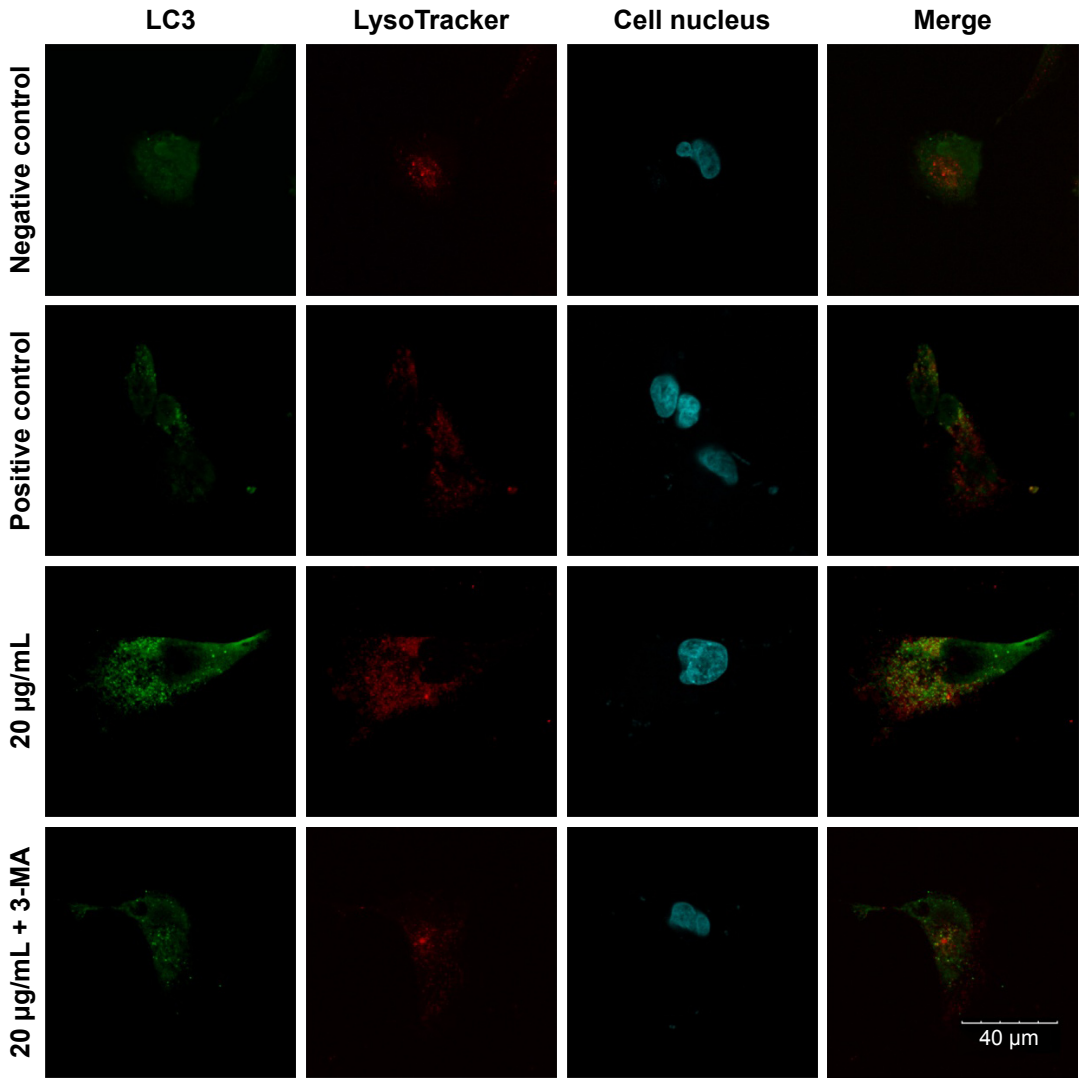

Figure 4 Confocal immunofluorescence images.
Notes: The MC3T3-E1 cells were cultured with 20 μg/mL Ta-NPs for 24 h, with or without pretreatment with 3-MA (10 mM) for 1 h; cells treated with α-MEM alone served as a negative control group, and cells treated with 200 nM rapamycin served as a positive control group. The LC3-labeled green puncta (a characteristic of autophagosomes) could be clearly observed in the positive control group and in the 20 μg/mL Ta-NP-treated group but were nearly indistinguishable in the negative control group. When cells were pretreated with 3-MA, the amount of green puncta decreased sharply. Experiments were repeated three times. Scale bar: 40 μm. Magnification ×1,200.
Abbreviations: 3-MA, 3-methyladenine; α-MEM, alpha-modified Eagle's medium; Ta-NPs, Ta nanoparticles.

alone. Collectively, these results illustrated that Ta-NPs could induce autophagy in the MC3T3-E1 cells and that 3-MA inhibited the Ta-NP-induced autophagy.

Expression of autophagy proteins

Autophagy was then detected via Western blotting to analyze the protein expression of autophagy markers, LC3B and p62 (Figure 5). As shown, an increase in the intensity of the LC3-II band and a decrease in the intensity of the p62 band were observed in the rapamycin-treated and 20 μg/mL Ta-NP-treated groups compared with the negative control group, while pretreatment with 3-MA accordingly weakened the LC3-II band intensity and enhanced the p62 band intensity (Figure 5A). Similarly, an analysis based on the gray value ratios revealed that the LC3-II/LC3-I level was significantly higher ($P<0.001$), and the p62/actin level was slightly lower ($P<0.05$) in the rapamycin-treated and 20 μg/mL Ta-NP-treated groups than those in the negative control group (Figure 5B). When pretreated with 3-MA, the LC3-II/LC3-I level decreased ($P<0.01$) and the p62/actin level increased ($P<0.05$), with significant differences compared with the group treated with Ta-NPs alone (Figure 5B). These results revealed that Ta-NP treatment upregulated the LC3-II expression and downregulated the p62 expression, which again indicated autophagy induction by the Ta-NPs in the MC3T3-E1 cells. The observed downregulation of LC3 and the upregulation of p62 resulted from the inhibition of Ta-NP-induced autophagy by 3-MA.

Ultrastructure of autophagic vesicles

Finally, we used TEM to observe the ultrastructure of autophagic vesicles to provide direct evidence of autophagy induction and autophagy inhibition (Figure 6). As presented in Figure 6, the autophagic vesicles (isolated membrane, autophagosomes, and autophagolysosomes) could be clearly observed both in the rapamycin-treated (Figure 6A) and 20 μg/mL Ta-NP-treated (Figure 6B and C) cells. Some autophagosomes even contained organelles, such as an endoplasmic reticulum. When pretreated with the autophagy inhibitor 3-MA (Figure 6D), the Ta-NPs could still be taken up by MC3T3-E1 osteoblasts and internalized in the cells but without autophagic vesicle formation instead of mitochondrial swelling. These results provided direct evidence that MC3T3-E1 osteoblasts underwent autophagy when treated with 20 μg/mL Ta-NPs. Pretreatment with 3-MA inhibited Ta-NP-induced autophagy and led to organelle damage, indicating that autophagy plays a protective role in cell survival.

Discussion

Porous Ta has been widely applied as a biomedical implant material and has exhibited excellent bone osseointegration and osseoincorporation. During loading wear, Ta-NPs may inevitably be released from the surface of implants and influence the cell behavior of peri-implant osteoblasts. Osteoblasts are some of the most active cells involved in bone remodeling and play an important role in the balance between bone formation and resorption. Therefore, it is of

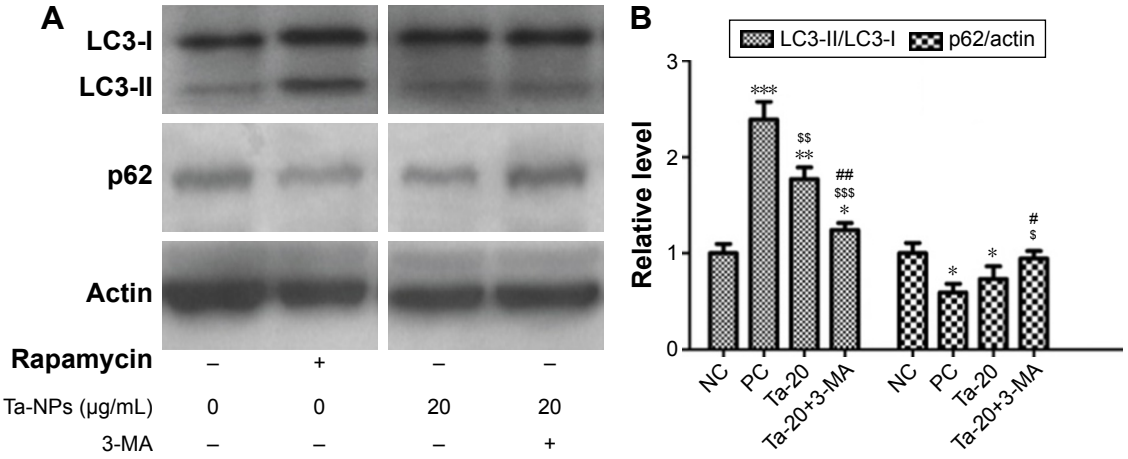

Figure 5 Expression of autophagy proteins by Western blots.

Notes: The MC3T3-E1 cells were cultured with 20 μg/mL Ta-NPs for 24 h, with or without pretreatment with 3-MA (10 mM) for 1 h; cells treated with α-MEM alone served as a negative control group, and cells treated with 200 nM rapamycin served as a positive control group. β-actin was used as the internal control. Compared to the negative control group, 20 μg/mL Ta-NPs treatment increased the LC3-II expression and decreased the p62 expression, while pretreatment with 3-MA counteracted the effect of Ta-NPs. Experiments were repeated three times. "NC" represents the negative control group, and "PC" represents the positive control group. $^{*}P<0.05$, $^{**}P<0.01$, $^{***}P<0.001$ versus negative control group; $^{\$}P<0.05$, $^{\$\$}P<0.01$, $^{\$\$\$}P<0.001$ versus positive control group; $^{\#}P<0.05$, $^{\#\#}P<0.01$ versus Ta-NPs alone treated group.

Abbreviations: 3-MA, 3-methyladenine; α-MEM, alpha-Modified Eagle's Medium; Ta-NPs, Ta nanoparticles.

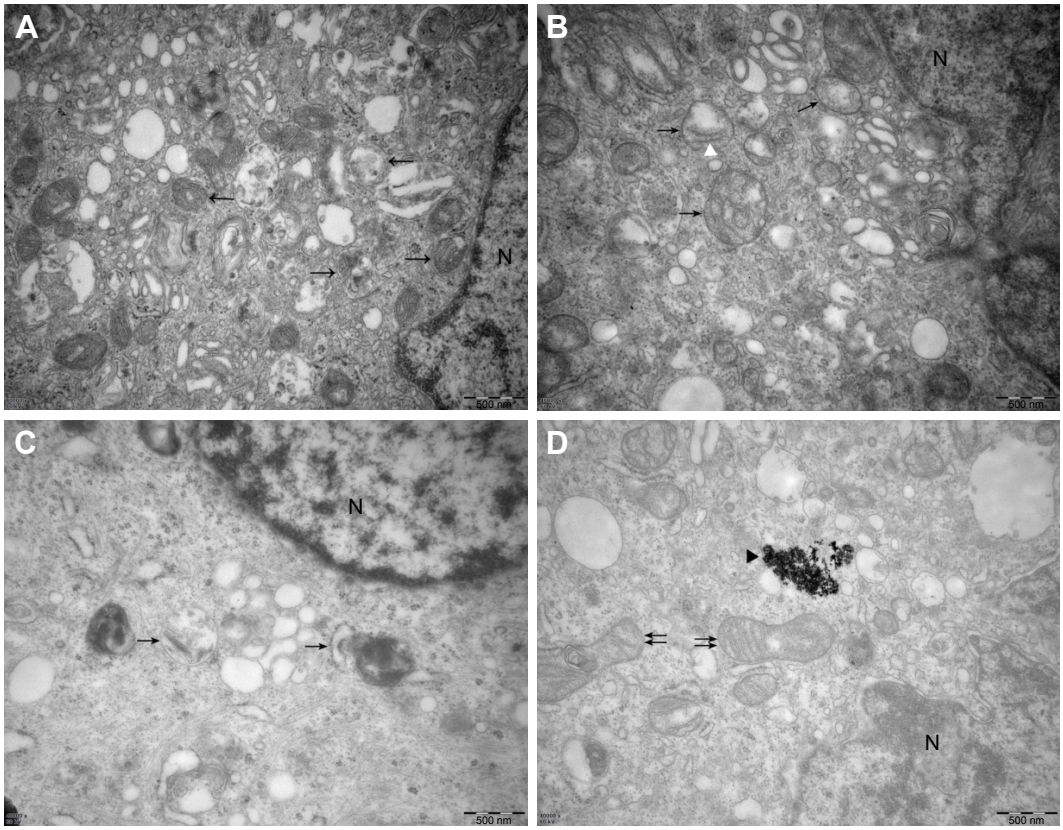

Figure 6 Ultrastructure of MC3T3-E1 cells imaged by TEM. The MC3T3-E1 cells were cultured with 20 μg/mL Ta-NPs for 24 h, with or without pretreatment with 3-MA (10 mM) for 1 h; cells treated with 200 nM rapamycin served as a positive control group.

Notes: In the rapamycin (**A**) and 20 μg/mL Ta-NP-treated (**B** and **C**) cells, the autophagic vesicles (isolated membrane, autophagosomes and autophagolysosomes; arrowheads) could be clearly observed, some even containing organelles such as an endoplasmic reticulum (white triangle). When the cells were pretreated with 3-MA (**D**), the Ta-NPs could still be taken up by MC3T3-E1 osteoblasts (black triangle), but without autophagic vesicle formation instead of mitochondrial swelling (double arrowheads). Scale bars: 500 nm. Magnification ×40,000. Arrowheads: autophagic vesicles; white triangle: endoplasmic reticulum; black triangle: internalized Ta-NPs; double arrowheads: swollen mitochondria; N: nucleus.

Abbreviations: 3-MA, 3-methyladenine; TEM, transmission electron microscopy; Ta-NPs, Ta nanoparticles.

great importance to investigate the interaction of Ta-NPs with osteoblasts for better regulation of the peri-implant bone remodeling.

Studies have shown that compared with non-bionic or non-porous materials, the cell adhesion, spreading, proliferation, differentiation, and mineralization of osteoblasts MC3T3-E1 were remarkably enhanced on honeycomb films or porous inorganic scaffolds, especially those with smaller pores.[30–32] Many studies have investigated the interaction of osteoblasts with porous Ta, Ta discs, and Ta coatings, but limited research has been performed on the interaction of osteoblasts with Ta-NPs. Ninomiya et al[14] compared the effects of various implant surfaces (Ti mesh, cobalt-chromium beads, and porous Ta) on osteoblast proliferation and found that the osteoblast proliferation on porous Ta was significantly greater than that on the other surfaces, thus revealing porous Ta as a superior scaffold. In this study, porous Ta was the most suitable implant surface among these three surfaces. However, the question of whether the porous structure, the Ta itself or both play a key role remains unclear. Balla et al[3] compared the performance of porous Ta and porous Ti and concluded that Ta was a superior material based on an identical porous structure. Similarly, a Ta coating on a Ti implant resulted in a more osseointegrative cell behavior than that of a Ti implant, as shown by improved osteoblast adhesion, increased cell proliferation and differentiation, decreased apoptosis in vitro, and enhanced bone healing efficacy in vivo.[33] In addition, a nanocrystalline Ta surface possessed higher surface hydrophilicity and enhanced corrosion resistance than those of conventional coarse-grained Ta.[34] Therefore, it was interesting to study how uncombined Ta nanoparticles behave. In the present study, MC3T3-E1 osteoblasts were cultured with 1, 10, and 20 μg/mL uncombined Ta-NPs, revealing that the cell viability increased compared with that of the untreated group, indicating that Ta-NPs can also promote osteoblast proliferation.

Then, we determined whether Ta-NPs could induce autophagy using confocal immunofluorescence images, Western blots, and TEM images. Autophagy is a complicated catabolic pathway that regulates the lysosomal degradation of unnecessary organelles and foreign bodies to maintain cell homeostasis, thus playing a cytoprotective role in cell growth, survival, proliferation, and differentiation.[35–37] Any extracellular factors can be recognized as foreign and can be taken up by cells through a number of membrane-mediated mechanisms in which the foreign bodies are internalized in lysosomes, endosomes, or autophagosomes.[38,39] In the initial stage of autophagy, a small vesicular sac called an isolation membrane elongates and subsequently encloses a portion of the cytoplasm and then forms a double-membraned structure called an autophagosome. LC3, a microtubule-associated protein 1 light chain 3, has four isoforms, among which LC3B is the most widely used (LC3 is simply referred to as LC3B in this paper).[40] LC3 is disposed at its C terminus and becomes LC3-I. The cytosolic form of non-lipidated LC3-I is converted to lipidated LC3-II, which tightly associates with both the outer and inner membranes of autophagosomes. Then, the autophagosome fuses with a lysosome to form an autolysosome. LC3 on the outer membrane is cleaved off, and LC3 on the inner membrane, together with the enclosed materials, is degraded, resulting in a very low LC3 content in the autolysosome.[40,41] Then, p62, a specific substrate that is preferentially degraded by autophagy, selectively joins the autophagosomes by directly binding to LC3, which is inversely correlated with autophagy activity.[40] Therefore, LC3 and p62 can be used as markers of autophagy.

In the present study, positive LC3 puncta, high LC3-II expression, and the autophagic vacuole ultrastructure were observed and identified as indicators of autophagy induction. Studies have reported that autophagy can be induced by various nanoparticles in osteoblasts, can promote the differentiation and mineralization of osteoblasts,[36,42] can protect osteoblasts from oxidative damage and apoptosis,[43] and can play essential roles in bone homeostasis.[44] Our present results indicate that Ta-NPs should be added to this nanoparticle list.

To confirm the hypothesis that autophagy was involved in Ta-NP-induced cell proliferation, the CCK-8 assay was conducted again to compare the cell viability of MC3T3-E1 osteoblasts when pretreated with or without an autophagy inducer (rapamycin) and autophagy inhibitor (3-MA). Rapamycin is an accepted classical autophagy inducer,[40] and 3-MA is a type-III phosphatidylinositol 3-kinase [PI-3K] inhibitor, which blocks the formation of autophagosomes (the initial stage of autophagy).[45] In the present study, treatment with rapamycin or 3-MA alone had no significant influence on cell viability, which was consistent with previous studies revealing that pretreatment with rapamycin (no more than 2 μM) or 3-MA (no more than 10 mM) had no significant influence on cell viability, differentiation, mineralization, apoptosis of osteoblasts, or the expression of autophagy and osteogenesis-related factors.[23,37,46,47] The cell viability further increased when the cells were pretreated with rapamycin but obviously decreased when they were pretreated with 3-MA, revealing that autophagy was involved in the Ta-NP-induced cell proliferation and had a promoting effect. This statement is consistent with the finding that nano-TiO_2-induced autophagy played a protective role against oxidative stress and promoted cell proliferation.[48]

When cells were pretreated with 3-MA, the reduction in cell viability was more visible in the 20 μg/mL Ta-NP-treated group (to 50% viability) than in the 10 μg/mL Ta-NP-treated group (to 80% viability), which may have resulted from the relatively high autophagy level in the 20 μg/mL Ta-NP-treated group. Autophagy, also known as self-eating, is a cellular response to external stimuli and plays a protective role in cell survival.[49] Limited self-eating can provide cells with the metabolic substrates needed to meet their energetic demands under stressful conditions or can favor the selective elimination of external stimuli.[49] However, once the autophagy threshold is exceeded, which means that the protection from autophagy has reached its limit, cell death is inevitable if harmful factors persist.[37] In MC3T3-E1 osteoblasts, basal autophagy occurs at a low level to ensure physiological homeostasis. When treated with Ta-NPs at a relatively low concentration of 10 μg/mL, the MC3T3-E1 osteoblasts could remain in a compensatory stage, with a 20% increase in cell viability, while autophagy remained below the threshold. As the concentration of Ta-NPs increased to 20 μg/mL, the autophagy level accordingly increased to better protect cells from external stimuli, with an 18.7% increase in cell viability. Once the protection of autophagy was completely inhibited by 3-MA, the cell viability was significantly decreased to 50%. Thus, if the Ta-NP concentration continues to increase and eventually exceeds the autophagy threshold, then the cell viability may decrease linearly. These results provide further evidence that autophagy plays protective roles in cell survival but within its threshold range.

Finally, we confirmed the inhibition of autophagy by 3-MA through confocal immunofluorescence images, Western blotting, and TEM images and found that the autophagy flux decreased, as shown by the reduced positive

LC3 puncta, reduced LC3-II expression, and disappearance of the autophagic vacuole ultrastructure instead of organelle damage, such as swollen mitochondria. These results clearly reveal that the decreased cell viability following 3-MA pretreatment was due to autophagy inhibition, which led to organelle damage, and the results further imply a promoting role of autophagy in cell proliferation.

Conclusion

In summary, the present study reported that Ta-NPs can promote the proliferation of MC3T3-E1 osteoblasts and induce autophagy. In addition, Ta-NP-induced autophagy promoted cell proliferation. However, further research is needed to explore the molecular mechanisms and signaling pathways through which Ta-NPs induce autophagy, which will be the focus of our next work.

Acknowledgments

This work was supported by the National Natural Science Foundation of China (51672122), the Natural Science Foundation of Guangdong Province (2015A030313299, 2016A030313673), the Development of Science and Technology of Guangdong Province Special Fund (2016A020215154), the Zhejiang Provincial Natural Science Foundation of China (LY16H140003), and the Wenzhou Municipal Science and Technology Bureau Foundation of China (Y20150070).

Disclosure

The authors report no conflicts of interest in this work.

References

1. Liu X, Song X, Zhang P, Zhu Z, Xu X. Effects of nano tantalum implants on inducing osteoblast proliferation and differentiation. *Exp Ther Med*. 2016;12(6):3541–3544.
2. Balla VK, Banerjee S, Bose S, Bandyopadhyay A. Direct laser processing of a tantalum coating on titanium for bone replacement structures. *Acta Biomater*. 2010;6(6):2329–2334.
3. Balla VK, Bodhak S, Bose S, Bandyopadhyay A. Porous tantalum structures for bone implants: fabrication, mechanical and in vitro biological properties. *Acta Biomater*. 2010;6(8):3349–3359.
4. Zhu Y, Gu Y, Qiao S, Zhou L, Shi J, Lai H. Bacterial and mammalian cells adhesion to tantalum-decorated micro-/nano-structured titanium. *J Biomed Mater Res A*. 2017;105(3):871–878.
5. Zhang D, Wong CS, Wen C, Li Y. Cellular responses of osteoblast-like cells to 17 elemental metals. *J Biomed Mater Res A*. 2017;105(1):148–158.
6. Findlay DM, Welldon K, Atkins GJ, Howie DW, Zannettino AC, Bobyn D. The proliferation and phenotypic expression of human osteoblasts on tantalum metal. *Biomaterials*. 2004;25(12):2215–2227.
7. Zardiackas LD, Parsell DE, Dillon LD, Mitchell DW, Nunnery LA, Poggie R. Structure, metallurgy, and mechanical properties of a porous tantalum foam. *J Biomed Mater Res*. 2001;58(2):180–187.
8. Bencharit S, Byrd WC, Altarawneh S, et al. Development and applications of porous tantalum trabecular metal-enhanced titanium dental implants. *Clin Implant Dent Relat Res*. 2014;16(6):817–826.
9. Liu Y, Bao C, Wismeijer D, Wu G. The physicochemical/biological properties of porous tantalum and the potential surface modification techniques to improve its clinical application in dental implantology. *Mater Sci Eng C Mater Biol Appl*. 2015;49:323–329.
10. Wang Q, Zhang H, Li Q, et al. Biocompatibility and osteogenic properties of porous tantalum. *Exp Ther Med*. 2015;9(3):780–786.
11. Tang Z, Xie Y, Yang F, et al. Porous tantalum coatings prepared by vacuum plasma spraying enhance bmscs osteogenic differentiation and bone regeneration in vitro and in vivo. *PLoS One*. 2013;8(6):e66263.
12. Smith JO, Sengers BG, Aarvold A, Tayton ER, Dunlop DG, Oreffo RO. Tantalum trabecular metal – addition of human skeletal cells to enhance bone implant interface strength and clinical application. *J Tissue Eng Regen Med*. 2014;8(4):304–313.
13. Sagomonyants KB, Hakim-Zargar M, Jhaveri A, Aronow MS, Gronowicz G. Porous tantalum stimulates the proliferation and osteogenesis of osteoblasts from elderly female patients. *J Orthop Res*. 2011;29(4):609–616.
14. Ninomiya JT, Struve JA, Krolikowski J, Hawkins M, Weihrauch D. Porous ongrowth surfaces alter osteoblast maturation and mineralization. *J Biomed Mater Res A*. 2015;103(1):276–281.
15. Bencharit S, Byrd WC, Hosseini B. Immediate placement of a porous-tantalum, trabecular metal-enhanced titanium dental implant with demineralized bone matrix into a socket with deficient buccal bone: a clinical report. *J Prosthet Dent*. 2015;113(4):262–269.
16. Papi P, Jamshir S, Brauner E, et al. Clinical evaluation with 18 months follow-up of new PTTM enhanced dental implants in maxillo-facial post-oncological patients. *Ann Stomatol (Roma)*. 2014;5(4):136–141.
17. Wei X, Zhao D, Wang B, et al. Tantalum coating of porous carbon scaffold supplemented with autologous bone marrow stromal stem cells for bone regeneration in vitro and in vivo. *Exp Biol Med (Maywood)*. 2016;241(6):592–602.
18. Fu WM, Yang L, Wang BJ, et al. Porous tantalum seeded with bone marrow mesenchymal stem cells attenuates steroid-associated osteonecrosis. *Eur Rev Med Pharmacol Sci*. 2016;20(16):3490–3499.
19. Jamil K, Chua KH, Joudi S, Ng SL, Yahaya NH. Development of a cartilage composite utilizing porous tantalum, fibrin, and rabbit chondrocytes for treatment of cartilage defect. *J Orthop Surg Res*. 2015;10:27.
20. Zhou R, Xu W, Chen F, et al. Amorphous calcium phosphate nanospheres/polylactide composite coated tantalum scaffold: facile preparation, fast biomineralization and subchondral bone defect repair application. *Colloids Surf B Biointerfaces*. 2014;123:236–245.
21. Schlee M, Pradies G, Mehmke WU, et al. Prospective, multicenter evaluation of trabecular metal-enhanced titanium dental implants placed in routine dental practices: 1-year interim report from the development period (2010 to 2011). *Clin Implant Dent Relat Res*. 2015;17(6):1141–1153.
22. Schlee M, van der Schoor WP, van der Schoor AR. Immediate loading of trabecular metal-enhanced titanium dental implants: interim results from an international proof-of-principle study. *Clin Implant Dent Relat Res*. 2015;17(Suppl 1):e308–e320.
23. Wang Z, Liu N, Liu K, et al. Autophagy mediated CoCrMo particle-induced peri-implant osteolysis by promoting osteoblast apoptosis. *Autophagy*. 2015;11(12):2358–2369.
24. Bonutti PM, Pivec R, Issa K, et al. Delamination of tantalum porous coating from a TKA due to regional dissemination of debris. *Orthopedics*. 2013;36(8):600–604.
25. Yu L, Lu Y, Man N, Yu SH, Wen LP. Rare earth oxide nanocrystals induce autophagy in HeLa cells. *Small*. 2009;5(24):2784–2787.
26. Peynshaert K, Manshian BB, Joris F, et al. Exploiting intrinsic nanoparticle toxicity: the pros and cons of nanoparticle-induced autophagy in biomedical research. *Chem Rev*. 2014;114(15):7581–7609.
27. Li H, Li Y, Jiao J, Hu HM. Alpha-alumina nanoparticles induce efficient autophagy-dependent cross-presentation and potent antitumour response. *Nat Nanotechnol*. 2011;6(10):645–650.

28. Stern ST, Adiseshaiah PP, Crist RM. Autophagy and lysosomal dysfunction as emerging mechanisms of nanomaterial toxicity. *Part Fibre Toxicol*. 2012;9:20.
29. O'Neill SC, Queally JM, Devitt BM, Doran PP, O'Byrne JM. The role of osteoblasts in peri-prosthetic osteolysis. *Bone Joint J*. 2013;95-B(8):1022–1026.
30. Wu XH, Wu ZY, Qian J, et al. Photo-crosslinked hierarchically honeycomb-patterned/macroporous scaffolds of calcium phosphate cement promote MC3T3-E1 cell functions. *Rsc Advances*. 2015;5(45):36007–36014.
31. Wu XH, Wang SF. Integration of photo-crosslinking and breath figures to fabricate biodegradable polymer substrates with tunable pores that regulate cellular behavior. *Polymer*. 2014;55(7):1756–1762.
32. Wu X, Wang S. Biomimetic calcium carbonate concentric microgrooves with tunable widths for promoting MC3T3-E1 cell functions. *Adv Healthc Mater*. 2013;2(2):326–333.
33. Wang L, Hu X, Ma X, et al. Promotion of osteointegration under diabetic conditions by tantalum coating-based surface modification on 3-dimensional printed porous titanium implants. *Colloids Surf B Biointerfaces*. 2016;148:440–452.
34. Huo WT, Zhao LZ, Yu S, Yu ZT, Zhang PX, Zhang YS. Significantly enhanced osteoblast response to nano-grained pure tantalum. *Sci Rep*. 2017;7:40868.
35. Zhao Y, Howe JL, Yu Z, et al. Exposure to titanium dioxide nanoparticles induces autophagy in primary human keratinocytes. *Small*. 2013;9(3):387–392.
36. Kaluderovic MR, Mojic M, Schreckenbach JP, Maksimovic-Ivanic D, Graf HL, Mijatovic S. A key role of autophagy in osteoblast differentiation on titanium-based dental implants. *Cells Tissues Organs*. 2014;200(3–4):265–277.
37. Yang L, Meng H, Yang M. Autophagy protects osteoblasts from advanced glycation end products-induced apoptosis through intracellular reactive oxygen species. *J Mol Endocrinol*. 2016;56(4):291–300.
38. Ma X, Wu Y, Jin S, et al. Gold nanoparticles induce autophagosome accumulation through size-dependent nanoparticle uptake and lysosome impairment. *ACS Nano*. 2011;5(11):8629–8639.
39. Ha SW, Weitzmann MN, Beck GR Jr. Bioactive silica nanoparticles promote osteoblast differentiation through stimulation of autophagy and direct association with LC3 and p62. *ACS Nano*. 2014;8(6):5898–5910.
40. Mizushima N, Yoshimori T, Levine B. Methods in mammalian autophagy research. *Cell*. 2010;140(3):313–326.
41. Tsukahara T, Matsuda Y, Usui Y, Haniu H. Highly purified, multi-wall carbon nanotubes induce light-chain 3B expression in human lung cells. *Biochem Biophys Res Commun*. 2013;440(2):348–353.
42. Camuzard O, Santucci-Darmanin S, Breuil V, et al. Sex-specific autophagy modulation in osteoblastic lineage: a critical function to counteract bone loss in female. *Oncotarget*. 2016;7(41):66416–66428.
43. Yang YH, Li B, Zheng XF, et al. Oxidative damage to osteoblasts can be alleviated by early autophagy through the endoplasmic reticulum stress pathway – implications for the treatment of osteoporosis. *Free Radic Biol Med*. 2014;77:10–20.
44. Nollet M, Santucci-Darmanin S, Breuil V, et al. Autophagy in osteoblasts is involved in mineralization and bone homeostasis. *Autophagy*. 2014;10(11):1965–1977.
45. Seglen PO, Gordon PB. 3-Methyladenine: specific inhibitor of autophagic/lysosomal protein degradation in isolated rat hepatocytes. *Proc Natl Acad Sci U S A*. 1982;79(6):1889–1892.
46. Kim IR, Kim SE, Baek HS, et al. The role of kaempferol-induced autophagy on differentiation and mineralization of osteoblastic MC3T3-E1 cells. *BMC Complement Altern Med*. 2016;16(1):333.
47. Yang JY, Park MY, Park SY, et al. Nitric oxide-induced autophagy in MC3T3-E1 cells is associated with cytoprotection via AMPK activation. *Korean J Physiol Pharmacol*. 2015;19(6):507–514.
48. Zhang X, Yin H, Li Z, Zhang T, Yang Z. Nano-TiO2 induces autophagy to protect against cell death through antioxidative mechanism in podocytes. *Cell Biol Toxicol*. 2016;32(6):513–527.
49. Galluzzi L, Vicencio JM, Kepp O, Tasdemir E, Maiuri MC, Kroemer G. To die or not to die: that is the autophagic question. *Curr Mol Med*. 2008;8(2):78–91.